

a combination of 9.4 cm of polarization maintaining (PM) single-mode fiber followed by 2.1 cm of polarization-maintaining HNF. Within the HNF assembly, pulses undergo a solitonic compression followed by the formation of a red-shifted soliton centered at a wavelength of 2 μm and an ultrabroadband dispersive wave around 1 μm . A variable insertion of material in the silicon prism sequence allows fine tuning of the dispersive wave to an optimum seed spectrum for the subsequent Yb: fiber stages. The final pulse duration is limited solely by the gain narrowing in the amplifiers. To avoid nonlinear effects, a grating stretcher employing a multilayer dielectric reflection grating with 1760 lines per millimeter is used to induce a group delay dispersion of approximately 20 ps^2 . The pulse duration is measured to be 1 ns before amplification. The beam is then coupled into a preamplifier consisting of a PM Yb:doped bulk fiber with a core diameter of 6 μm . This stage is pumped bidirectionally with a total optical power of 1.9 W at a wavelength of 975 nm by pigtailed single-mode pump diodes. The pump light is combined with the seed through wavelength division multiplexers. All components of the system are PM to avoid polarization mode dispersion. The output spectrum obtained after pre-amplification at full pumping power is depicted in Fig. 2(c). The resulting average output is 696 mW, indicating a total gain of 27 dB. The pulse is centered at a wavelength of 1.03 μm with a full width half-maximum (FWHM) bandwidth of 14.7 nm, corresponding to a transform-limited duration of 81 fs. Figure 2(a) shows the average output as a function of seed power. The preamplifier operates in saturation starting from 0.2 mW, which is less than 20% of the available total seed power. A free-space optical isolator protects the preamplifier from reflections occurring in the following stages of the system.

The main amplification is obtained in a 1.5-m-long single-mode Yb-doped double-clad PCF with airclad technology [13] and a large signal core diameter of 40 μm (aeroGAIN-FLEX 1.5, NKT Photonics). Stress-applying parts and a coiling diameter of 30 cm ensure stable polarizing operation with high beam quality. As a pump source, we use two fiber-coupled multi-mode laser

diodes with wavelength stabilization at 974.8 nm. A total of 103 W of optical power is coupled into the PCF in counter-propagating direction. A dichroic mirror combines signal and pump light. Figure 2(c) shows the measured spectrum after the PCF at maximum pump power. It is centered at a wavelength of 1.033 μm with a bandwidth of 11.4 nm (FWHM), corresponding to a transform limit of 125 fs. Note a minor gain narrowing with respect to the preamplification stage. The residual background due to amplified spontaneous emission is 40 dB below the peak intensity. Even under full pumping power, the spectrum does not show any nonlinear distortion effects. The average output as a function of pump power is depicted in Fig. 2(b). A total output of 72 W is achieved. This value corresponds to a gain of 20.1 dB with slope efficiency of 72.7%. At this point, the pulse energy is as high as 7.2 μJ at our repetition rate of 10 MHz.

We employ specially designed multilayer dielectric reflection gratings for recompressing the pulses [14], identical to those used in the stretcher. The diffraction efficiency is higher than 95% over the full spectral bandwidth around 1.03 μm . A total throughput of the compressor of more than 83% results in output pulses with energies of 6 μJ . The final transverse mode quality is remarkable, with an M^2 better than 1.4 measured for both axes.

To characterize the pulse properties after compression, we retrieve second-harmonic generation frequency-resolved optical-gating (SHG-FROG) data [15] at full output power. Figure 3(a) shows the measured amplitude envelope, whereas Fig. 3(b) depicts the reconstructed trace. The temporal intensity profile of the pulses and its phase is shown in Fig. 3(c) yielding a FWHM pulse duration of 145 fs. The quality of the FROG reconstruction is underlined by the agreement of the direct output spectrum in Fig. 2(c) with the reconstructed spectral intensity in Fig. 3(d). A peak power of 36.8 MW is calculated from the measured pulse shape and energy. This value allows for intensities up to 10^{15} W/cm^2 under diffraction-limited focusing, opening up interesting

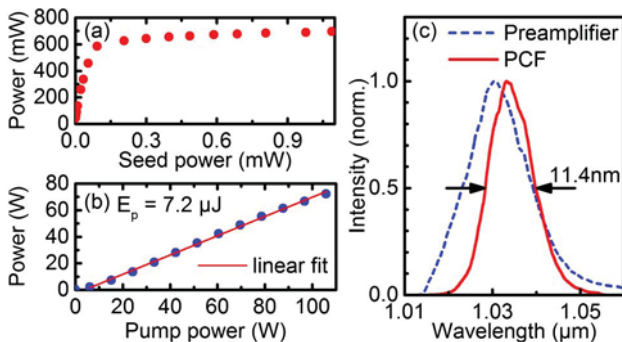


Fig. 2. (a) Output power of the Yb: fiber preamplifier as a function of seed power. The maximum average power amounts to 696 mW, and saturation is clearly visible. (b) Average power after the photonic crystal fiber amplifier as a function of pump power. The slope efficiency is 72.7%. (c) Spectrum after pre-amplifier (blue dashed) and after main amplifier (solid red), corresponding to a pulse energy of 7.2 μJ before compression at a repetition rate of 10 MHz.

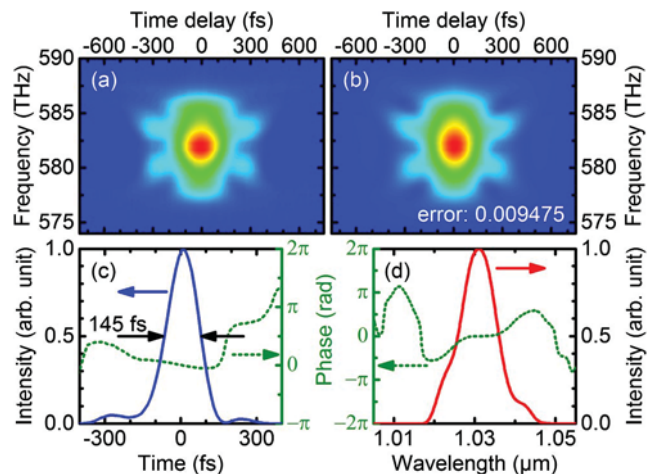


Fig. 3. SHG FROG measurement of compressed 6 μJ pulses. (a) Amplitude of measured FROG trace (128×128 pixels); (b) retrieved FROG trace in amplitude with 0.0095 reconstruction error; (c) intensity and phase profile as a function of time; (d) spectral intensity and phase.

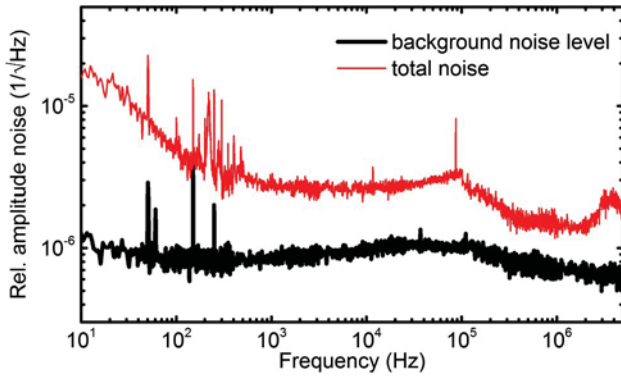


Fig. 4. Noise performance of the high power fiber amplifier. Relative amplitude noise spectrum (red line) and corresponding electronic detection noise floor (black line).

applications in extremely nonlinear optics [8] and sub-cycle quantum manipulation of light [16].

For the advanced applications we target, low amplitude noise and long-term stability represent key features of the laser source. We therefore took special care about designing a robust setup not requiring any active stabilization mechanisms. For this reason, we inspected the noise performance of the entire system under normal laboratory conditions using an InGaAs photodiode. Figure 4 shows the relative amplitude noise measured by a spectrum analyzer with frequency components from 10 Hz up to the 5-MHz Nyquist frequency. The amplitude noise remains below $2 \cdot 10^{-5} \text{ Hz}^{-1/2}$ for the entire frequency range studied. A value as low as $1.5 \cdot 10^{-6} \text{ Hz}^{-1/2}$ is obtained at 1 MHz. A two-hour long-term stability measurement was performed by detecting the pulse train with a lock-in amplifier set to the 10-MHz reference frequency at a time constant of 30 ms. The results are depicted in Fig. 5(a). Excellent power stability is proved by an rms standard deviation as small as $2.78 \cdot 10^{-4}$. A long-term test of the system is shown in Fig. 5(b) highlighting relative power drifts lower than 0.3% over three days of continuous operation.

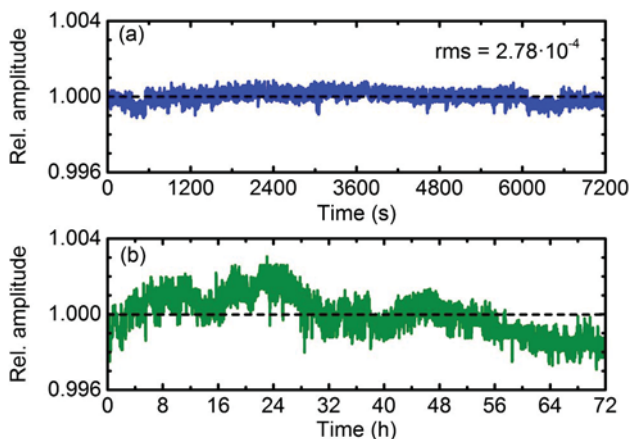


Fig. 5. Stability measurements of the linear CPA system performed at full output: (a) average power measured by lock in amplifier over two hours with time constant set to 30 ms and readout every 100 ms (72001 data points); (b) long term stability measured over 3 days of continuous operation, acquisition every 5 s with a calibrated photodiode (51269 data points).

We stress that a parallel arm of the Er: fiber seed system generates up to 500-nm-broad spectra in another highly nonlinear fiber. These pulses are characterized by a constant carrier-envelope phase. They may be compressed down to pulse durations of 7 fs [9,17] and are intrinsically synchronized to the pulses from the Yb: amplifier. In addition, a synchronously driven Tm: fiber amplifier system [12] provides the opportunity for coherent synthesis of single-cycle pulses in the μJ energy range [18]. These capabilities underline the extreme flexibility of our approach.

In conclusion, an Yb: fiber amplifier seeded by an Er: fiber system delivers $6\text{-}\mu\text{J}$ pulses with duration of 145 fs at a repetition rate of 10 MHz. Its noise performance and long-term stability achieve levels that, to our knowledge, are unprecedented by any femtosecond technology operating at high average power. In addition, the passive phase locking and inherent synchronization to ultrabroadband few-cycle pulses provided by the Er: seed and a parallel Tm: fiber amplifier branch represent attractive features for advanced experiments in extreme nonlinear optics, sub-cycle quantum physics, and ultrafast spectroscopy with ultimate sensitivity in general.

This work has been supported by the European Research Council (ERC) via the Advanced Grant “Ultra-Phase” (ERC-2011-AdG No. 290876), by Zukunftskolleg, by EC through the Marie Curie CIG project “UltraQuEsT” No. 334463 and by BW Stiftung Eliteprogramm.

References

1. C. Jauregui, J. Limpert, and A. Tünnermann, *Nat. Photonics* **7**, 861 (2013).
2. P. Russell, *Science* **299**, 358 (2003).
3. T. Eidam, J. Rothhardt, F. Stutzki, F. Jansen, S. Hädrich, H. Carstens, C. Jauregui, and A. Tünnermann, *Opt. Express* **19**, 255 (2011).
4. A. Ruehl, A. Marcinkevicius, M. E. Feermann, and I. Hartl, *Opt. Lett.* **35**, 3015 (2010).
5. Y. Kobayashi, N. Hirayama, A. Ozawa, T. Shukegawa, T. Seki, Y. Kuramoto, and S. Watanabe, *Opt. Express* **21**, 12865 (2013).
6. A. Fernández, K. Jespersen, L. Zhu, L. Grüner Nielsen, A. Baltuška, A. Galvanauskas, and A. J. Verhoef, *Opt. Lett.* **37**, 927 (2012).
7. D. Mortag, T. Theeg, K. Hausmann, L. Grüner Nielsen, K. Giessmann Jespersen, U. Morgner, D. Wandt, D. Kracht, and J. Neumann, *Opt. Commun.* **285**, 706 (2012).
8. A. Cingöz, D. C. Yost, T. K. Allison, A. Ruehl, M. E. Fermann, I. Hartl, and J. Ye, *Nature* **482**, 68 (2012).
9. D. Brida, G. Krauss, A. Sell, and A. Leitenstorfer, *Laser Photonics Rev.* **8**, 409 (2014).
10. F. Röser, J. Rothhardt, B. Ortac, A. Liem, O. Schmidt, T. Schreiber, J. Limpert, and A. Tünnermann, *Opt. Lett.* **30**, 2754 (2005).
11. G. Krauss, D. Fehrenbacher, D. Brida, C. Riek, A. Sell, R. Huber, and A. Leitenstorfer, *Opt. Lett.* **36**, 540 (2011).
12. S. Kumkar, G. Krauss, M. Wunram, D. Fehrenbacher, U. Demibras, D. Brida, and A. Leitenstorfer, *Opt. Lett.* **37**, 554 (2012).
13. K. P. Hansen, C. B. Olausson, J. Boerg, D. Noordegraaf, M. D. Maack, T. T. Alkeskjold, M. Laurila, T. Nikolajsen, P. M. W. Skovgaard, M. H. Sørensen, M. Denninger, C. Jakobsen, and H. R. Simonsen, *Opt. Eng.* **50**, 111609 (2011).

14. M. D. Perry, R. D. Boyd, J. A. Britten, D. Decker, B. W. Shore, C. Shannon, and E. Shults, *Opt. Lett.* **20**, 940 (1995).
15. D. J. Kane and R. Trebino, *IEEE J. Quantum Electron.* **29**, 571 (1993).
16. C. Riek, J. Schmidt, S. Eckart, D. V. Seletskiy, and A. Leitenstorfer, *CLEO* (Postdeadline Paper Digest), OSA Technical Digest (online) (Optical Society of America, 2014), paper FTh5 A.6.
17. A. Sell, G. Krauss, R. Scheu, R. Huber, and A. Leitenstorfer, *Opt. Express* **17**, 1070 (2009).
18. G. Krauss, S. Lohss, T. Hanke, A. Sell, S. Eggert, R. Huber, and A. Leitenstorfer, *Nat. Photonics* **4**, 33 (2010).